Non-circular Chainring Optimization for In Phase Handcycling

Master Semester Worksheets

by Jonas Østergaard Juhl

Aalborg University
Department of Health Science and Technology
10^{th} semester Sports Technology
12th August 2013

Contents

About

This project is developed at the master semester of sports technology at Aalborg University, spring 2013. The project continues the work from the previous 9^{th} semester, and presents the main product, an article written on the basis of both semesters on the form of a scientific paper. Present worksheets starts out with an overview of the work carried out at the 9^{th} semester followed up by a detailed description of the work carried out at the master semester.

The 9^{th} semester report can be found at http://nejsumjuhl.dk/files/p9.pdf and will be available at least until the exam has passed.

A special thanks to:
Supervisor: Christian Gammelgaard Olesen.
the AnyBody Research Group for their software assistance and supervision.
Wolturnus A/S, for providing the contact to experienced handcyclists and practical work with the laboratory equipment.

Jonas Ø. Juhl
August 2013

Worksheet 1

9^{th} Semester Model

The previous 9^{th} semester project was about optimizing the planar geometrical shape of a non-circular chainring for lying in phase handcycling to perform better at olympic competitions. To overcome this problem an inverse dynamics driven musculoskeletal model of handcycling was established, and optimization of the crank velocity together with arm kinematics was conducted. However, it was impossible to interpret the optimization result to a chainring shape due to inadequately definition of the optimization problem, thus the optimization problem must be redefined in present project.

This worksheet gives a short description of the applied modeling of the 9^{th} semester project.

1.1 Musculoskeletal Modeling

The model was established with the commercial software *The AnyBody Modeling System v5.3.0*, AMS [1.1]. The human model was based on the *FreePostureHandSR* from the *AnyBody Managed Model Repository version 1.5* and was limited to the torso and upper extremities and the muscles acting to move the arms. A simple muscle model, possessing constant strength regardless of the situation, was applied. All joint positions of thorax were held constant and its joint loads were absorbed by external reaction forces, meaning that the muscles are doing no contractions to maintain the posture, i.e. thorax was simulated to a fully supported supine posture.

Despite the gravity of earth, an environmental model represented the crank-mechanism of the handcycle. The crank-mechanism was rotating around its axle causing the arms connected, via revolute joints, to the handles to move, see **fig. 1.1**. During the revolution, the human muscles must outbalance the force generated by a torque at the crank-axle.

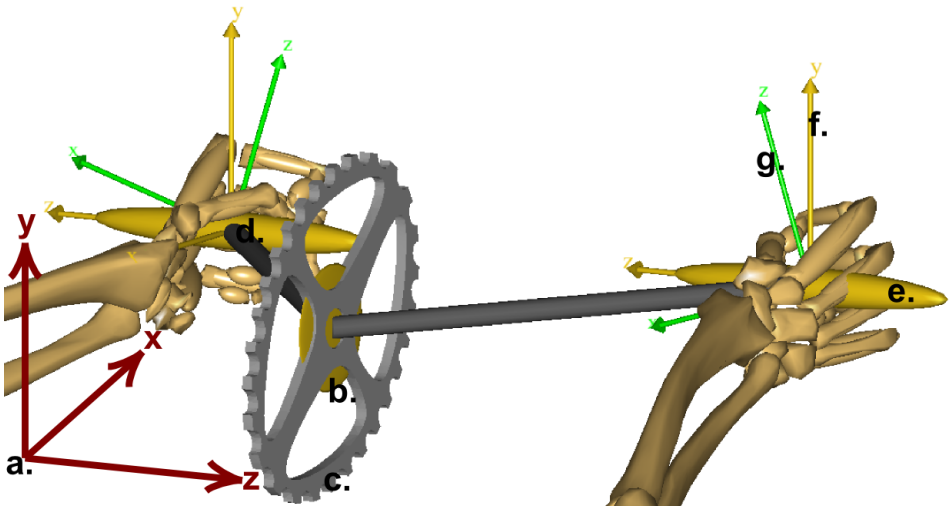

Figure 1.1: Illustration of the Crank-mechanism. *a*: The orientation of the global reference system. *b*: a *Wheel* segment rotating by θ_{lin}. *c*: An *AdditionalCrank* segment rotating by θ_{add} relative to the *Wheel* segment. *d*: A reference node of the *AdditionalCrank* segment. *e*: A handle segment. *f*: A reference system of a handle segment. *g*: Hands are grasping the z-axes of these reference systems.

References

[1.1] *http://www.anybodytech.com/*. 10.08.2013.

Worksheet 2

Master Semester Plan

The previous 9^{th} semester project did not result in a successful complete report. First of all, the report intendently lacked model validation, and secondly, an erroneous result indicated that the model optimization was not correctly defined. The overall plan for present project is to redefine the 9^{th} semester model optimization, followed by model validation.

When using musculoskeletal models, many assumptions must be taken and it is very difficult to maintain the overview of all their influences. Therefore, model validation must be performed before the result can be trusted, and this will be a major topic of present project.

At the previous 9^{th} semester model optimization the crank velocity of the chainring was intended to be continuously adjusted at every iteration of the optimization towards a better solution until a proper solution was found. Unfortunately the optimization revealed that the mean angular crank velocity was varying during the iterations implying that some error exists in the modeling. The error is identified in the way the angular crank velocity, ω is expressed. It was mistakenly assumed that if ω was just as much below the mean angular velocity as above, it would result in a constant mean angular crank velocity. This is not the case because it do not cause the additional angular position, θ_{add} ("the angular position" - ω·time) of the crank to be just as much below zero as above, which is essential in obtaining a constant mean angular crank velocity. Therefore, in present project it is the additional angular position of the crank which is optimized instead of its angular velocity as in the previous 9^{th} semester project.

The previous 9^{th} semester optimization relied on a weak assumption ensuring constant power throughout the crank revolution. The incentive to obey this assumption was vindicated by avoiding the very large air drag exposed at high translational velocities on the handcycle and cyclist. However, the cadence of handcycling is reasonably high about 100 rpm, the crank torque are smooth enough, and the inertia of the handcycle and cyclist are large enough to minimize the velocity variations during a revolution to insignifi-

cance. Therefore, present project will also implement the torque-curve to the optimization, enabling the musculoskeletal model to act more naturalistic.

The objective function of the previous 9^{th} semester optimization will also be improved, as a new one has just been suggested for bicycling in the literature.

Worksheet 3

Model Optimization Conduction

In the previous 9^{th} semester project the non-circular chainring radius and arm kinematics of the musculoskeletal model were optimized by the *Complex Method* [3.1]. As stated in *Worksheet 2* there was an error in the way the crank rotation was expressed, and the optimization might have been based on an assumption simplifying the problem too much. The criticized assumption prompted the crank power to be constant at any time during a pedal revolution, which is not necessarily naturalistic. The musculoskeletal model in present project will be the one used in the previous 9^{th} semester project but these two problems will be corrected. The improved optimization will enable the crank power to vary over a pedal revolution but maintain a constant mean power, unfortunately on the cost of more design variables increasing the complexity. Also the previous applied objective function, *peak maximum muscle activity*, has been substituted by an improved version taking both the peak maximum muscle activity and the integral of all muscle activities over one revolution into consideration.

This worksheet only describes the application of the *Complex Method* in present project, and will not dig into background knowledge as this was described in the previous 9^{th} semester project.

3.1 Design Variables

The angular crank position, θ, the glenohumeral abduction, $GHAbd$, and the crank torque, τ, are desired to be manipulated directly. The expression and design variables of the $GHAbd$ were successfully carried out in the previous 9^{th} semester project and will be done in the same way in present project by **eq. 3.1**.

$$GHAbd = \phi_{start} + \frac{0.5\phi_{def}}{l_{xHandle}} \cdot -yHub_{handle} \tag{3.1}$$

Where $l_{xHandle}$ is the distance in the global x-y plane from the crank axle center to the position of the handles, and $yHub_{handle}$ is the y-value of the handles in the rotated reference system of Hub. The ϕ_{start} and ϕ_{def} represents the starting angle and deflection of the $GHAbd$ and is illustrated in **fig. 3.1**. See also *Worksheet 1*, **fig. 1.1** for the x, y, and z orientations of the handles relative to the global reference sytem.

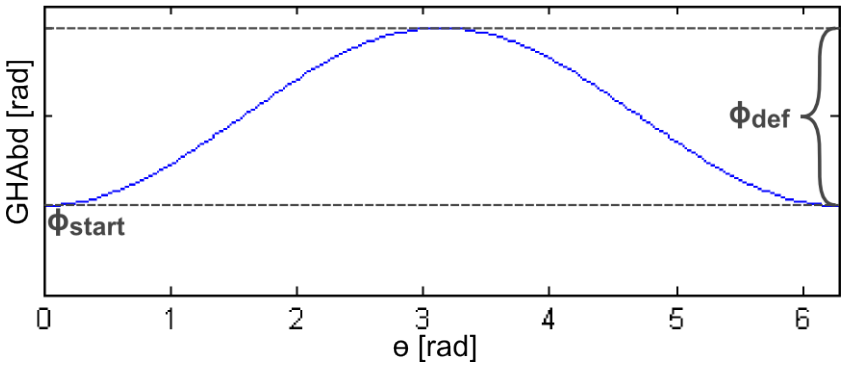

Figure 3.1: Example of the relationship between ϕ_{start} and ϕ_{def} in **eq. 3.1**, and glenohumeral abduction, relative to the crank angle.

The crank rotation in the previous 9^{th} semester model was incorrectly controlled by its angular velocity expressed by a sum of two sine functions and an offset. Instead, present project is controlling its angular position, θ. θ is splitted into two functions, **eq. 3.2**.

$$\theta = \theta_{Lin} + \theta_{Add} \tag{3.2}$$

Where θ_{Lin} is the angular crank position derived from the mean angular crank velocity, ω_{Mean}, **eq. 3.3**.

$$\theta_{Lin} = \omega_{Mean} t \tag{3.3}$$

With t being the time. θ_{Add} will be able to vary throughout the iterations of the optimization, and it shall possess the same value and slope in $t = 0$ and $t = T$, where T is the time to complete one revolution of the crank mechanism. This ensures that the analyzed revolution are able to repeat it self with more revolutions in series. This is carried out by expressing the θ_{Add} by a sum of two sine functions minus an offset, **eq. 3.4**. Note that this equation differs from that shown in the article, because it is intended to express positive ω's and θ's in the article, while this expression leads to negative ω's and θ's, and thereby also negative mechanical power for forward moving handcycling.

$$\theta_{Add}(t) = A_{\theta A} \cdot sin(\omega_{Mean} t + \varphi_{\theta A}) + A_{\theta B} \cdot sin(2\omega_{Mean} t + \varphi_{\theta B}) - Offset \quad (3.4)$$

Where the As (amplitudes) and φs (phases) are the four design variables of θ_{Add}. The $Offsets$ ensures that θ_{Add} starts in zero and is thereby given as the value in $t = 0$, **eq. 3.5**.

$$Offset = A_{\theta A} \cdot sin(\varphi_{\theta A}) + A_{\theta B} \cdot sin(\varphi_{\theta B}) \quad (3.5)$$

Expressing τ with the sum of sine functions and an offset is done well if it is expressed relative to θ instead of t. This is proper because the work done at one crank revolution is: $W = \tau \cdot \Delta\theta$, whereby it is ensured that W will be constant throughout every iteration of the optimization and equal to the mean torque, τ_{Mean}, times 2π. τ can then be defines as **eq. 3.6**.

$$\tau(\theta) = \tau_{Mean} + A_{\tau A} \cdot sin(\theta + \varphi_{\tau A}) + A_{\tau B} \cdot sin(2\theta + \varphi_{\tau B}) \quad (3.6)$$

Where the As (amplitudes) and φs (phases) are the four design variables of τ.

Now all the design variables have been defined, with four of them in the θ, another four in the τ, and two in the $GHAbd$, which then is a total of ten design variables. The previous 9^{th} semester optimization counted only 6 design variables so the computational demand have been very much enlarged by increasing the search space by 4 dimensions. However, it is not considered to cut out a sinus term of the θ or τ to reduce the number of design variables. This might have been fairly done in 180 *degrees out of phase* handcycling by assuming that the left side of the body is equal to the right side in regards to anthropometry, strength and motor control. But in present *in phase* handcycling the two terms of sine functions (rather than one term) in θ and τ permits any two diametrically opposite phases of the crank revolution to be unequal to each other, which is beneficial as fx the model may do the pull phase stronger or weaker than the push phase.

3.2 Objective Function

In the previous 9^{th} semester the optimization was minimizing the peak activity of the most active muscle curve over one crank revolution: $Minimize : Peak(MaxAct)$. This objective function minimized indeed the activity of the most active muscle over one revolution, but it could be at the cost of a lot of muscle metabolism. Therefore present project replace this objective function with the recently proposed objective function for level bicycling at preferred cadence [3.2].

$$Objective\ function = \int_0^T \sum (Activity^2) dt \quad (3.7)$$

Where $\sum(Activity^2)$ means the sum of all the muscle activities powered by two. Even though this objective function was based on bicycling it is assumed that it applies well to handcycling.

3.3 Simple Arm Model

The model is now very close to start running the optimization. But instead of initializing the optimization right away, wait for several months until it converges, and possible find out that the result is useless due to some incorrect model definition, a simple arm model is constructed to execute optimizations quickly and correct possible errors. The simple arm model will not be used to draw conclusions on its results, but just ensuring that the constrains are effective, the objective function is expressed correctly, and that no other lurking variable contaminates the optimization result.

The simple model consists of two segments and four muscles, representing a two dimensional right arm. An *upper arm* segment, is attached to the initial reference system by a cylindrical joint at the shoulder position, allowing translation and rotation around an axis lying perpendicular to the driving direction. The *upper arm* segment is linked to a *forearm* segment by a revolute joint representing the elbow, allowing rotation also about an axis lying perpendicular to the driving direction. The *forearm* segment are then linked to the right crank arm by a spherical joint. One muscle represents the posterior deltoid and provides glenohumeral flexion, while another muscle represents the posterior deltoid and provides glenohumeral extension. Yet another muscle represents the biceps brachii and provides elbow flexion, while another muscle represents the triceps brachii and provides elbow extension. The simple arm model and muscle origin and insertion points are seen on **fig. 3.2**.

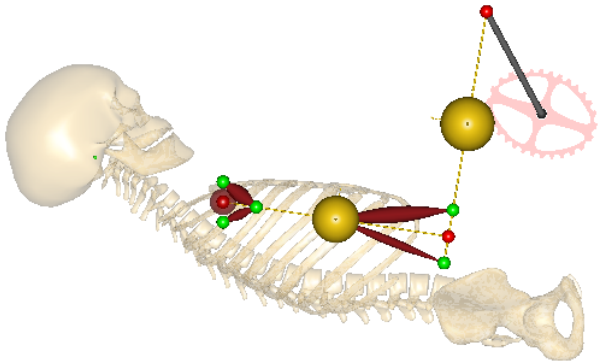

Figure 3.2: Illustration of the simple arm model. The location of the head and torso of the detailed model are shown as the transparent skeleton. The crank-mechanism are shown in the right top corner. The thin yellow lines and the big yellow spheres is the segments and segment masses. The small red spheres are the joints. The dark red fusiform objects are the muscles, and the small green spheres are its origin and insertion points.

With the simple arm model an iteration is completed in 2 seconds, whereby an optimization converges in about 2 hours, and this was used to correct a couple of errors before initializing the detailed musculoskeletal model.

3.4 Initial Settings and Results

Here follows the initial settings and results of the optimization of the detailed musculoskeletal model. The population size of the *Complex Method* is set to 20. The *Complex Method* is unconstrained except for the $GHAbd$ and θ. The θ_{start} is given a lower limit of 0.087 radians, and θ_{def} is given a lower limit of 0, which is necessary to avoid the elbows to penetrate the ribcage during pedaling. The angular crank velocity is constrained to always be greater than 3.4 rad/s, Ensuring the minimum radius of the finally derived chainring shape to be large enough to fit standard crank spiders. The initial box sizes are defined for every design variable to:

$A_{\theta A}$: 1
$\varphi_{\theta A}$: 1
$A_{\theta B}$: 1
$\varphi_{\theta B}$: 1
$A_{\tau A}$: 5
$\varphi_{\tau A}$: 5
$A_{\tau B}$: 1
$\varphi_{\tau B}$: 1
θ_{Start}: 0.14

θ_{Def}: 0.14

The stopping criteria's tolerances of the objective function and design variables are both set to 10^{-5}. Another stopping criteria stopped the optimization study if the number of iterations exceeded 4000.

Four optimization studies with different initial guesses of the design variables are executed, **tab. 3.4**.

	#1		#2		#3		#4	
	Initial	Opt.	Initial	Opt.	Initial	Opt.	Initial	Opt.
$A_{\theta A}$	0	6.5418e-1	0	-7.4524e-2	0.2	-5.9710e-1	0.2	5.3013e-1
$\varphi_{\theta A}$	0	-3.5874e-1	$\pi/2$	-3.1856e-2	$\pi/8$	1.2237e0	$\pi+\pi/2$	3.8872e0
$A_{\theta B}$	0	6.3252e-2	0	2.4422e-1	0.05	-4.1683e-2	0.05	1.5716e-3
$\varphi_{\theta B}$	0	-3.8035e0	$\pi+\pi/2$	4.4296e0	$\pi/2$	2.0113e0	$\pi+\pi/2$	3.5885e0
$A_{\tau A}$	0	-1.3590e1	0	-1.0973e1	0	1.1597e1	0	-4.7697e0
$\varphi_{\tau A}$	0	-1.6885e0	$\pi/2$	-4.4794e-1	$\pi/8$	4.8419e-1	$\pi+\pi/8$	3.5555e0
$A_{\tau B}$	0	1.5986e1	0	-2.3411e0	0	-2.5594e0	0	-3.2482e0
$\varphi_{\tau B}$	0	-1.8159e0	$\pi+\pi/2$	2.1218e0	$\pi/2$	1.5534e0	$\pi+\pi/2$	1.6537e0
θ_{Start}	0	-8.3594e-2	0	-8.8203e-2	0	-8.7916e-2	0	-8.7787e-2
θ_{Def}	0	6.1729e-1	0	1.0438e-1	0	1.0011e0	0	1.0194e0
Obj	**-**	**0.79**	**-**	**1.20**	**-**	**0.83**	**-**	**0.88**

Table 3.1: The initial and optimized values of the design variables and the related objective function value. Note that the A's are with opposite sign than that shown in the article, as it is desired to express positive ω's in the article.

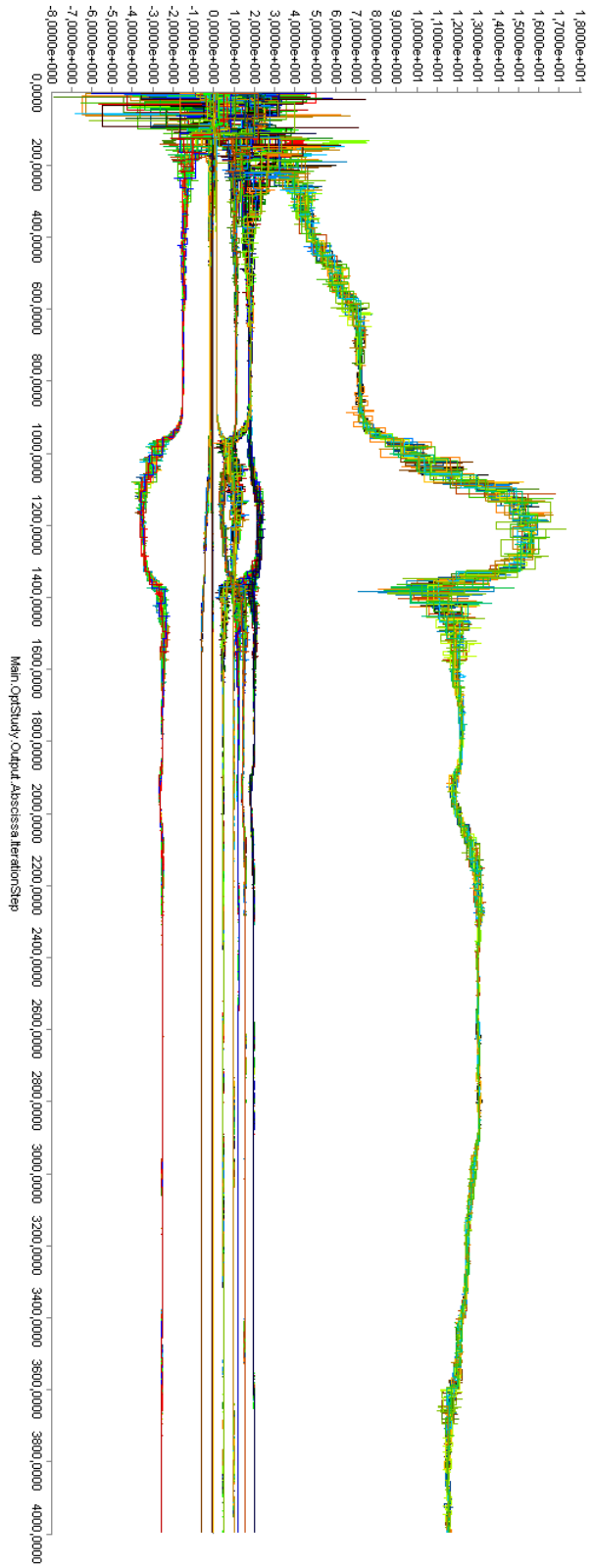

Figure 3.3: A graph showing the design variables being optimized. A population of 20 for every design variable of optimization study #3 relative to the number of iterations.

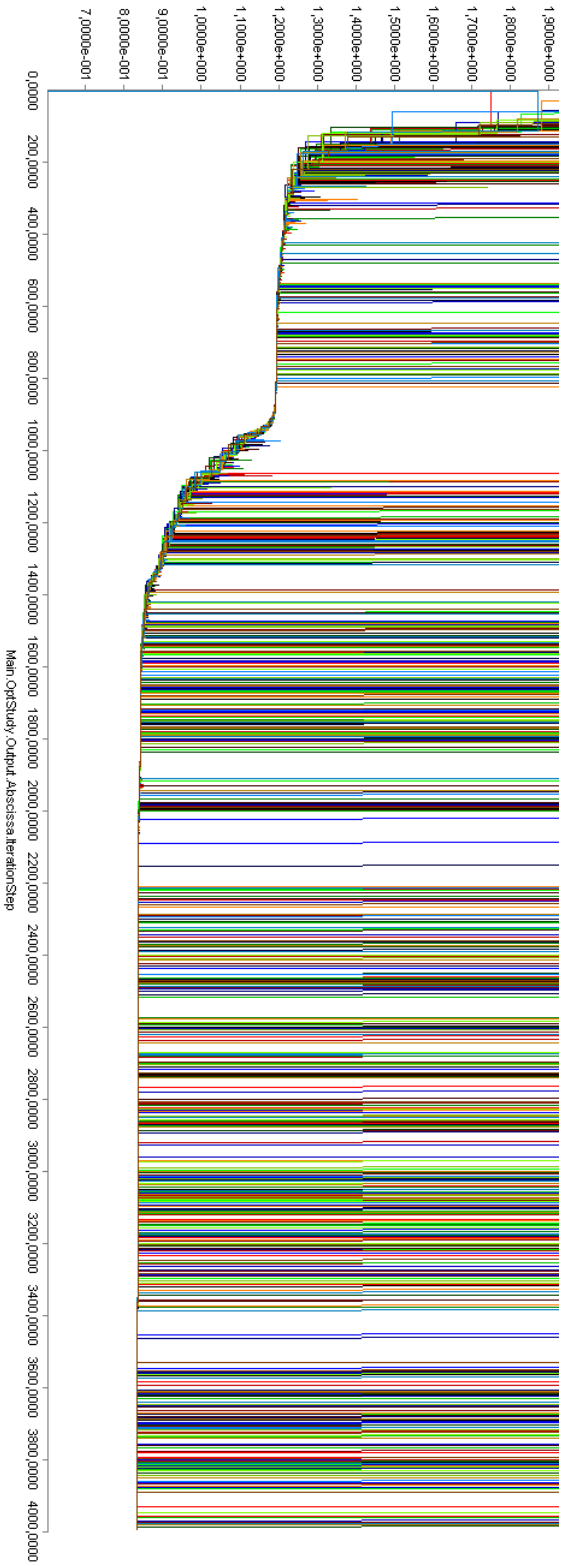

Figure 3.4: The objective function values for the population (of 20) of the optimization study #3, relative to iterations. An abrupt vertical increase in the objective function are shown every time the optimization study violates constrains.

The ω's of the optimization results are shown in **fig. 3.5**

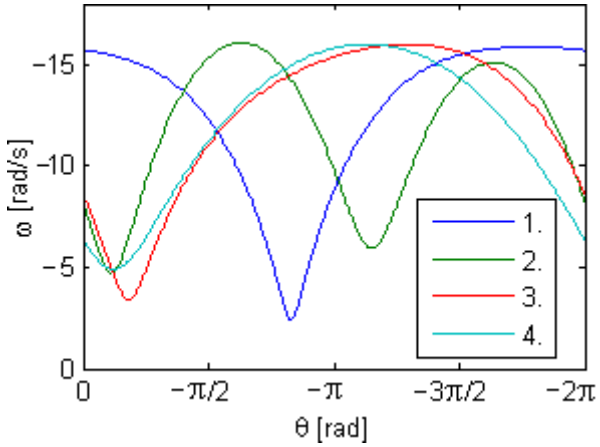

Figure 3.5: The ω's of the four optimization studies with different initial starting values.

References

[3.1] Guin J. A., *Modification of the Complex method of constraint optimization.* 1968, Computer Jornal, 10, 416-417. [3.2] Saeed Davoudabadi Farahani, *titel xxx.* 2013, Aalborg University, Still unpublished.

Worksheet 4

Optimization Result Interpretation

As seen on **fig. 3.5** in worksheet 3, the optimization studies found very different solutions, indicating that the objective function is very concave in nature. Therefore, it can not be assumed that the truly optimum is found. Optimization #1 and #3 show the best objective function values, and were therefore investigated further. It is desired to design chainrings which meet the optimized ω's. This is not possible because the chain wraps around the chainring, thus its larger radii will sooner or later get in the way and increase the intended chainring radius as the chain has to wrap around these larger radii as well. Alternative mechanisms, which can meet the optimized ω's more accurately can be used, such as shown on **fig. 4.1**.

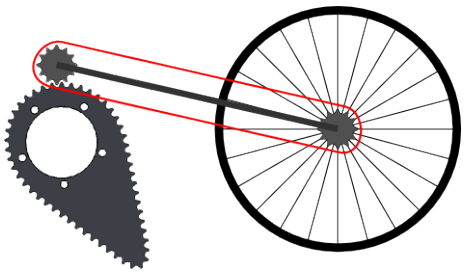

Figure 4.1: Illustration of an alternative drive-mechanism, which is able to meeet the optimized *omega*'s more accurately.

The drive-mechanism shown above is able to meet any optimized ω profile within a small error margin, and it may even work with slightly concave chainrings. However, the drive-mechanism involve an extra gear interaction than the conventional drive-mechanism, which leads to more frictional losses and a heavier solution. Therefore, the optimized ω profiles are met best possible by non-circular chainrings and a conventional drive-mechanism.

If not the chain had to wrap around the whole chainring, as in **fig. 4.1**, the variable chainring radius can be expressed as **eq. 4.1**.

$$r_{simple} = \frac{v_{chain}}{\omega} \tag{4.1}$$

where v_{chain} is the chain velocity. It is assumed that the cadence and kinetic energy of the handcyclist and handcycle is so high that the v_{chain} is well approximated to be constant. Thereby, the v_{chain} is given as **eq. 4.2**.

$$v_{chain} = r_{mean} \cdot \omega_{mean} = r_{mean} \cdot \frac{-2 \cdot \pi}{T} \tag{4.2}$$

Where r_{mean} is the radius of a 52-toothed circular chainring (0.105 m).The r_{simple} of optimization study 1 and 3 can be drawn with polar coordinates as shown on **fig. 4.2**.

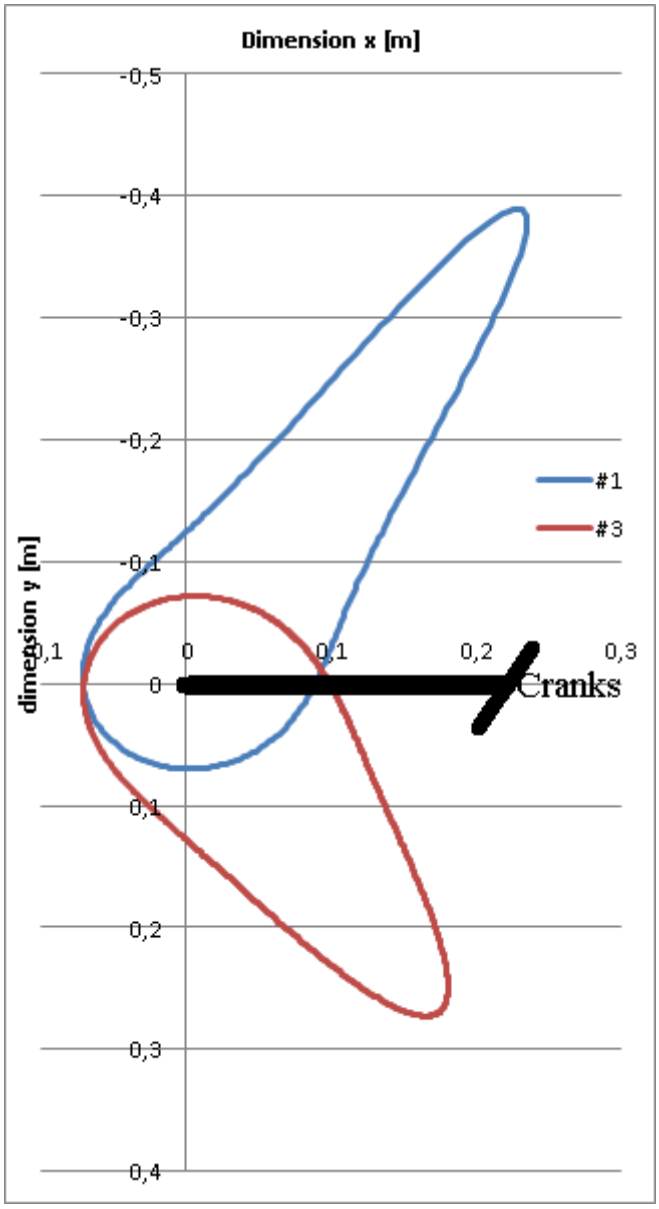

Figure 4.2: Polar plot of the r_{simple}, illustrating the shape and starting position of the chainrings. The chainrings rotates clockwise about origo, and theoretically interacts with the chain in the lowest point of intersection with the vertical axis. The cranks are oriented parallel to a line, intersecting the hub and a point midway between shoulders with the handlebars located furthest away from the shoulders, ready to start the pull phase.

The chainrings shown on **fig. 4.2** have mean radii larger than r_{mean}. This can be accounted for by shifting the gear to a higher sprocket. However, it is

desired to keep the number of tooths constant, and therefore the chainrings on **fig. 4.2** will be downscaled. A simple downscaling will just multiply a factor to the r_{simple}, but that will cause the smallest radii to become too small, making the chainrings unable to fit standard spider arms with a bolt circle diameter of 110 mm. The minimum radius the chainring can be, while still fitting a standard spider arm is 0.068723 m. Therefore, the r_{simple} is downscaled so that its radii closest to 0.068723 m are scaled the least, and the largest radii are scaled the most, by **eq. 4.3**.

$$r = (r_{simple} - 0.068723m) \cdot c + 0.068723m \tag{4.3}$$

Where c is the scaling factor ensuring the circumference of the chainrings to be similar to 52-toothed circular chainring ($\pi \cdot 2 \cdot 0.105$). The circumferences of the chainrings are numerically calculated by the sum of 900 linear pieces the chainrings are split to, as **eq. 4.4**.

$$circumference = \sum \sqrt{(\Delta x)^2 + (\Delta y)^2} \tag{4.4}$$

Then the c of **eq. 4.3** is adjusted until the circumference is equal to $\pi \cdot 2 \cdot 0.105$, which gives c's of: 0.355 for #1, and 0.521 for #3. A drawing of the r of optimization #1 and #3 with polar coordinates are seen on **fig. 4.3**.

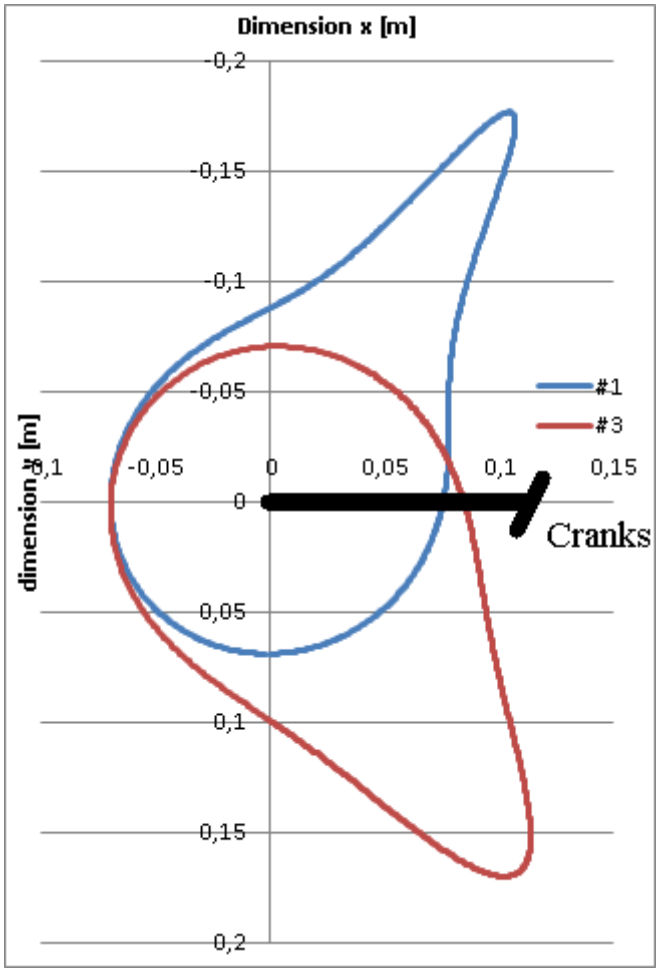

Figure 4.3: Polar plot of the r (the corrected r_{simple}). The chainrings rotates clockwise about origo, and theoretically interacts with the chain in the lowest point of intersection with the vertical axis. The cranks are oriented parallel to a line, intersecting the hub and a point midway between shoulders with the handlebars located furthest away from the shoulders, ready to do the pull phase.

The chainrings shown on **fig. 4.3** differs from their original shapes, and the angular crank velocity profile which will be produced by these chainrings will also differ from **fig. 3.5** in Worksheet 4. To make sure that the interpreted chainring designs still performs well, the angular crank velocities produced by these chainrings, will be derived and included in two new optimization studies, where only the torque- and glenohumeral abduction profiles are optimized. First the chain position relative to crank angle is estimated, see **fig. 4.4**.

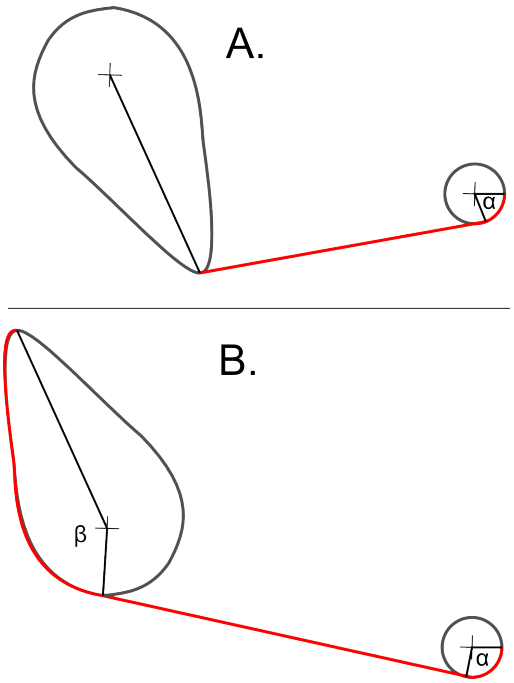

Figure 4.4: Example of the chain length of optimization study #3. A: the chain length (red) to crank angle = 0. B: the chain length to crank angle = π rad. The chain length is estimated to 28 different crank angles, by measuring the two angles α and β, and then calculate the length of the red curve. The red curve on the little sprocket wheel is calculated as a circular section, the freely hanging chain is given in vector coordinates and thereby calculated by phytagoras, and the red curve on the non-circular chainring is calculated by the previous shown **eq. 4.4**.

The estimated chain position relative to the crank angle is estimated as shown by **fig. 4.4**. It is desired to express the chain position relative to time instead of crank angle, so that it can be input to the musculoskeletal model. This is carried out with linear interpolation, which finds the chain position to a known time, between two known chain positions, see **fig. 4.5**.

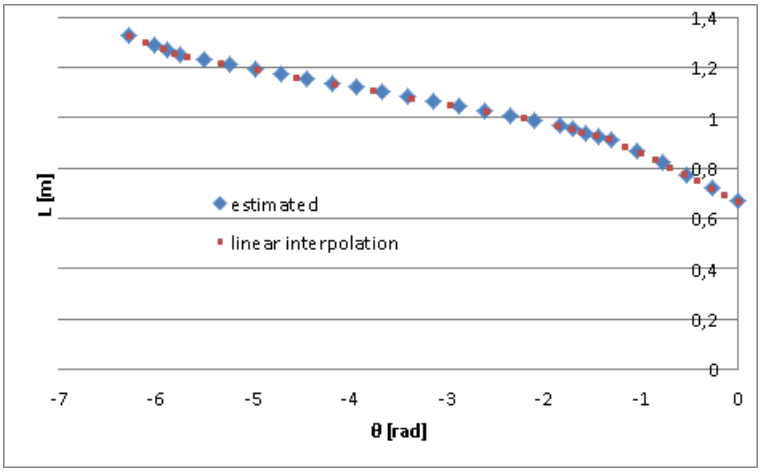

Figure 4.5: Example of optimization study #3. The estimated and interpolated chain position.

The chain position is then subtracted by $\omega_{mean}t$ to get the additional chainring position. The additional chain position is fitted to $\theta_{Add}(t) = A_{\theta A} \cdot sin(\omega_{Mean}t + \varphi_{\theta A}) + A_{\theta B} \cdot sin(2\omega_{Mean}t + \varphi_{\theta B}) - Offset$, see **fig. 4.6**.

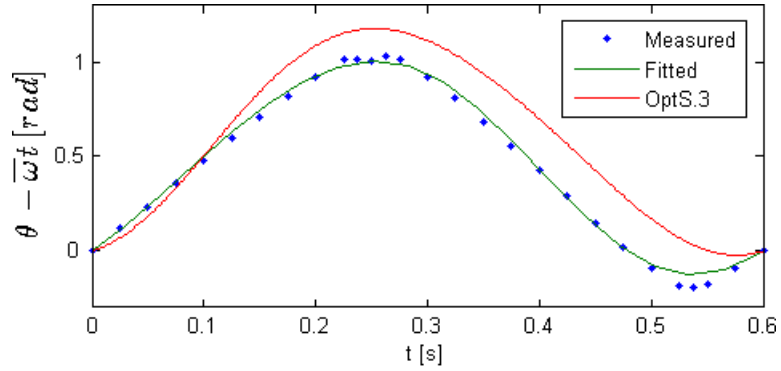

Figure 4.6: Showing the additional chain position of optimization #3 (blue dots), the fitted curve (green curve, and the optimized position data pre-interpretation (red curve). $A_{\theta A}$=-0.5621, $\varphi_{\theta A}$=0.9868, $A_{\theta B}$=-0.02645, and $\varphi_{\theta B}$=-0.5959. Note that the additional chain position is with opposite sign than that of the article, because it is desired to express positive crank angular velocities in the article.

Two new optimization studies of #1 and #3 are now launched, with only the torque- and glenohumeral abduction profiles as design variables. This is done, to see if the approximated chainring designs performs well. The additional crank angular velocity of #3 are replaced by the fittet curve from **fig. 4.6**. Because the #1 and #3 is very similar in shape, the #1 has

also its additional angular crank velocity replaced by the fittet curve from **fig. 4.6**, but phase shifted 1.12 radians. The box sizes of the optimization studies were halved, the population set to 12, while constrains and stopping criteria remained the same. The new optimization studies revealed even better objective function values of 0.73 and 0.74 for #1 and #3, respectively. These values are very similar, but the #3 chainring is the chosen design as the present maximum muscle activity over one crank revolution is only 50% compared to 55% for the #1. See **fig. 4.5** for the optimization results of the interpreted #3.

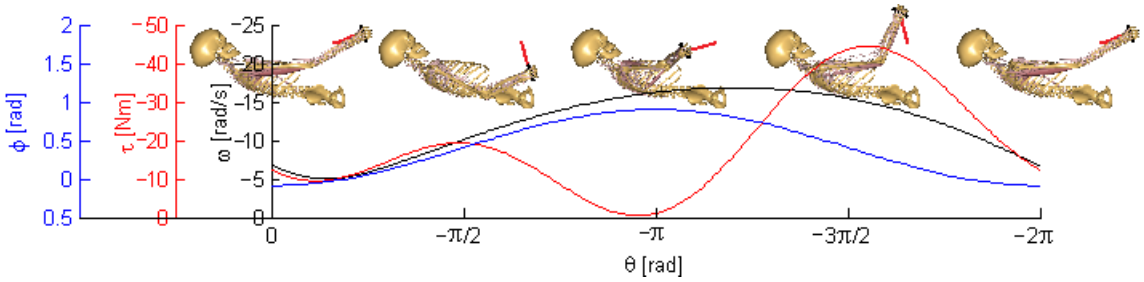

Figure 4.7: The new optimization result of #3 with the estimated chain position implemented. ϕ is glenohumeral abduction, τ is torque, and ω is the angular crank velocity.

Worksheet 5

Chainring Manufacturing

This worksheet documents the approach for drawing the optimized chainring followed by the production method.

5.1 Drawing

The picture of the optimized planar geometrical shape, **fig. 4.3** in worksheet 4 was imported to the 3D mechanical CAD program, *SolidWorks 2011*. Then the shape was approximately sketched by 52 linear pieces of 12.7 mm each, joined together at its ends to form a closed convex chain, see **fig. 5.1**. Every linear piece represents the orientations of the chain pitches. The slightly concavities are ignored, as the chain can not follow the chainring periphery in these gaps.

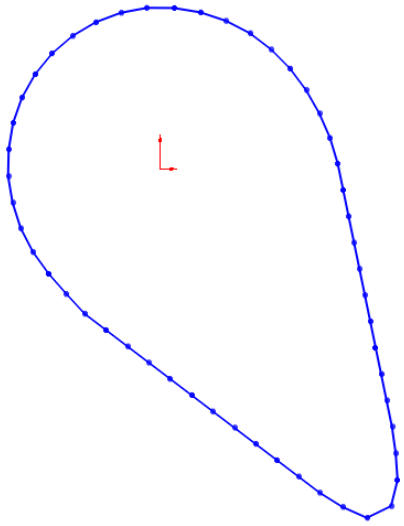

Figure 5.1: The joined 52 Linear Pieces, each representing the orientations of the chain pitches.

A picture of a real chainwheel was imported to *SolidWorks 2011* and this was used to estimate the tooth profile of one chain link by sections of circular arcs, see **fig. 5.2**.

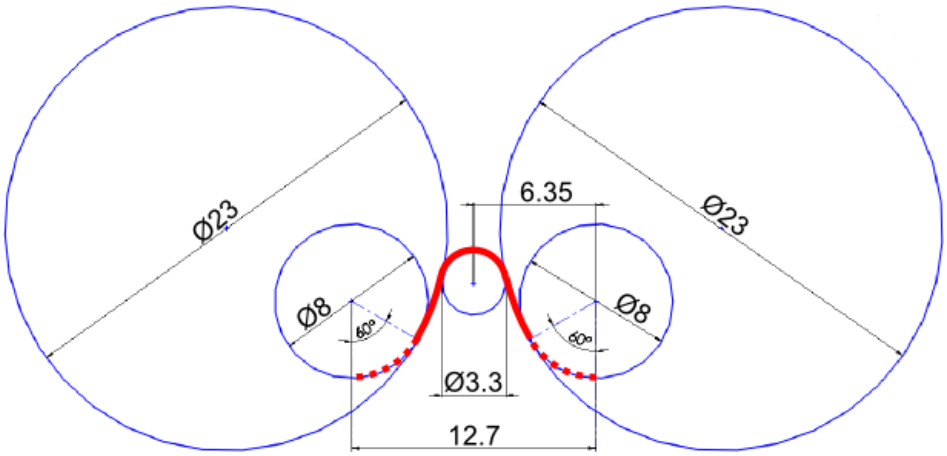

Figure 5.2: The tooth profile design of the optimized chainwheel in milimeters. The red curve is the actual tooth profile, whereof the dotted sections are the sections which will partly overlap when the 52 tooth profiles are joined together in their *Ø8* centers.

The estimated tooth profile was copied to 52 elements, and these replaced the linear pieces, by rotating / translating them in the plane until their *Ø8* circle centers were connected to the endpoints of the linear pieces, while making sure that the tooths are pointing outwards. The overlapping parts of the *Ø23* circles were deleted. 5 holes with *Ø10.5* where drawn equally distributed with their centers located at a circle of *Ø110* centered at the crank axle, with one of the holes placed 14.41 degrees below the positive x-axis. Finally a large *Ø94* hole was drawn with its center located at the crank axle, whereby the two dimensional drawing of the optimized chainring was completed, see **fig. 5.3**.

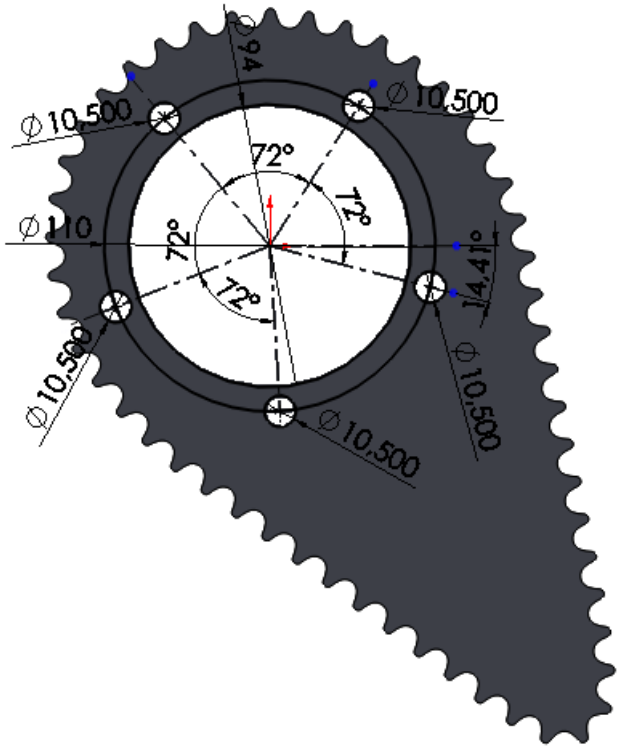

Figure 5.3: The tooth profile design of the optimized chainring in millimeters. The red curve is the actual tooth profile, and the dotted sections are the sections which will partly overlap when the 52 tooth profiles are joined together in their *Ø8* centers.

5.2 Manufacturing

The optimized chainring was produced in UDDEHOLM ARNE steel [5.1], which is an universal manganese-, chromium-, tungsten- alloy tool steel. The Chainring contour was cut by wire-cut Electric discharge machining, and the tooths were cut by CNC milling. Finally the tooths were sharpened with a hand held file. The process took place at the machine workshop affiliated to the institute of mechanics and production at Aalborg University.

References

[5.1] *http://www.uddeholm.dk/danish/files/Arne_datablad.pdf.* 10.08.2013.

Worksheet 6

Validation

This Worksheet provide further information about the validation experiment described in the article.

6.1 Experiment

The primary objective was to clarify if handcycling with the optimized chainring reduces steady state oxygen consumption, compared to a similar toothed circular chainring, when cycling at submaximal constant speed. This is done because the major portion of the energy delivered by the human body in road handcycling comes from the aerobic system, whereby oxygen uptake is the main limiting factor and a good measure of performance. Secondary, the maximal speed is tested with the optimized chainring design, compared to a circular. A randomized crossover design is used, where the randomization is carried out by writing *NON* on 5 equally sized slips of paper, and *CIR* on another 5 slips of paper. Then all ten slips of paper were shuffled on a table with the text facing downward, and then every subject was told to pick a slip of paper to determine which chainring to start with (NON = non-circular, CIR = circular).

Subjects
10 inexperienced male subjects participated in this study (see **tab. 6.1**) together with an elite subject (50.0 yr; 178 cm; 63 kg; 67.0 cm), who is a Paralympic competitor 2012, competing in the H3 class.

Subject	Group	Age (yr)	Height (cm)	Weight (kg)	Arm length (cm)
A	CIR	30.6	182.0	82.0	66.5
B	CIR	26.3	188.5	100.8	72.0
C	NON	28.0	185.6	81.0	70.0
D	CIR	27.9	177.0	76.0	65.5
E	NON	26.0	191.0	75.8	71.0
F	NON	26.2	182.0	70.0	63.5
G	CIR	26.1	185.5	83.2	69.5
H	NON	28.3	171.0	73.8	64.0
I	NON	26.1	185.5	87.0	74.5
J	CIR	32.4	180.0	89.4	67.0
Mean		27.8	182.8	81.9	68.4
SD		2.2	5.8	9.0	3.6

Table 6.1: Data of the 10 inexperienced subjects. The *Group* shows the starting chainring.

All subjects were orally informed about the objective and possible risks of their participation, and gave their written consent to participate (see **fig. 6.1**).

Forsøg med håndcykling med et noncirkulært kædehjul kontra et cirkulært kædehjul

Kontaktperson til dette forsøg
Jonas Østergaard Juhl
10. semester sportsteknologi, Aalborg Universitet
Tlf: 22 27 89 80
Email: joj08@student.aau.dk

Introduktion
Formålet med dette forsøg er at teste iltforbruget og den maksimale hastighed ved brug af et noncirkulært kædehjul i forhold til et cirkulært kædehjul til håndcykling.

Procedure
Testningen indebærer et enkelt besøg i sportslaboratoriet på Niels Jernes Vej 14, 9220 Aalborg, og har en varighed af 2 timer. Forsøgsprotokollen består af følgende:

1) 10 minutter opvarmning på håndcyklen med kædehjul A W
2) 4 minutter håndcykling med kædehjul A

3) 10 minutter opvarmning på håndcyklen med kædehjul B
4) 4 minutter håndcykling med kædehjul B

5) To maksimale hastighedsmålinger af ca. 15 sek varighed med kædehjul B

6) To maksimale hastighedsmålinger af ca. 15 sek varighed med kædehjul A

Under håndcyklingen vil data for: effekt, kadance, hastighed, og moment, blive indsamlet. I punkt 2) og 4) vil dine respirationsgasser blive målt med *Oxycon Pro Jaeger* via en maske, der sættes for munden. Data for din kropsvægt, højde, armlængde, fødselsdato, træningserfaring, og alkoholindtagelse de sidste 2 døgn vil ligeledes blive noteret.

Risici
Der er ingen signifikante risici forbundet med deltagelsen i dette forsøg.

Fortrolighed
Alt information, som indsamles under dit besøg holdes fortroligt og anonymt, og vil kun viderebringes med din tilladelse. Dine personlige oplysninger vildog altid kun være tilgængelige for dette forsøgs team.

Underskrift for samtykkerklæring
Med din underskrift indvilliger du i at alt information, der sindsamles under dit besøg må offentliggøres anonymt. Du kan når som helst trække dig ud af forsøget, men forsøgsteamet må da bruge din information op til det tidspunktet for tilbagetrækningen.

Deltagernavn:_____

Deltager underskrift: _____ Dato:_____

Forsøgsleders underskrift:_____ Dao:_____

Figure 6.1: The consent

Test Protocol

1. Put on the facemask of the pulmonary gas exchange recorder, but without the mouthpiece.
2. 10 min warm-up with either the non-circular or circular chainring. The subjects were told to keep a speed of 20 $km \cdot h^{-1}$, corresponding to 100 Watt and 55 rpm. However, two subjects had their speed, cadence, and mechanical power reduced, because they were not capable of completing the test protocol.
3. 2 min pause. Plug in the mouthpiece.
4. 4 min bout at the same speed.
5. 8 min pause, while the chainring was swapped, and the mouthpiece was plugged out.
6. 10 min Warm-up and adaption to the new chainring at 100 W and 55 rpm (except for the two subjects who had their intensity reduced).
7. 2 min pause. Plug in the mouthpiece.
8. 4 min bout at the same speed.
9. 6 min pause. The facemask was removed.
10. A maximal speed bout. The subjects accelerated steadily to a high speed over 20 s and then pedaled all out for about 10 s until the speed decreased.
11. 2 min pause.
12. A maximal speed bout, similar to the first one.
13. 8 min pause, while the chainring was swapped.
14. A similar maximal speed bout.
15. 2 min pause.
16. A similar maximal speed bout.

In the pauses the facemask was set up in the forehead and water was offered.

Experimental Setup

Here are shown some pictures of the laboratory setup described in the article.

Figure 6.2: A: shows the crank-mechanism with the cranks oriented in phase of each other. B: shows the driven front wheel loaded with a 15 m 8 kg copper cable to increase the kinetic energy. A 0.5 kg weight disc is also attached to the wheel to outbalance the weight distribution.

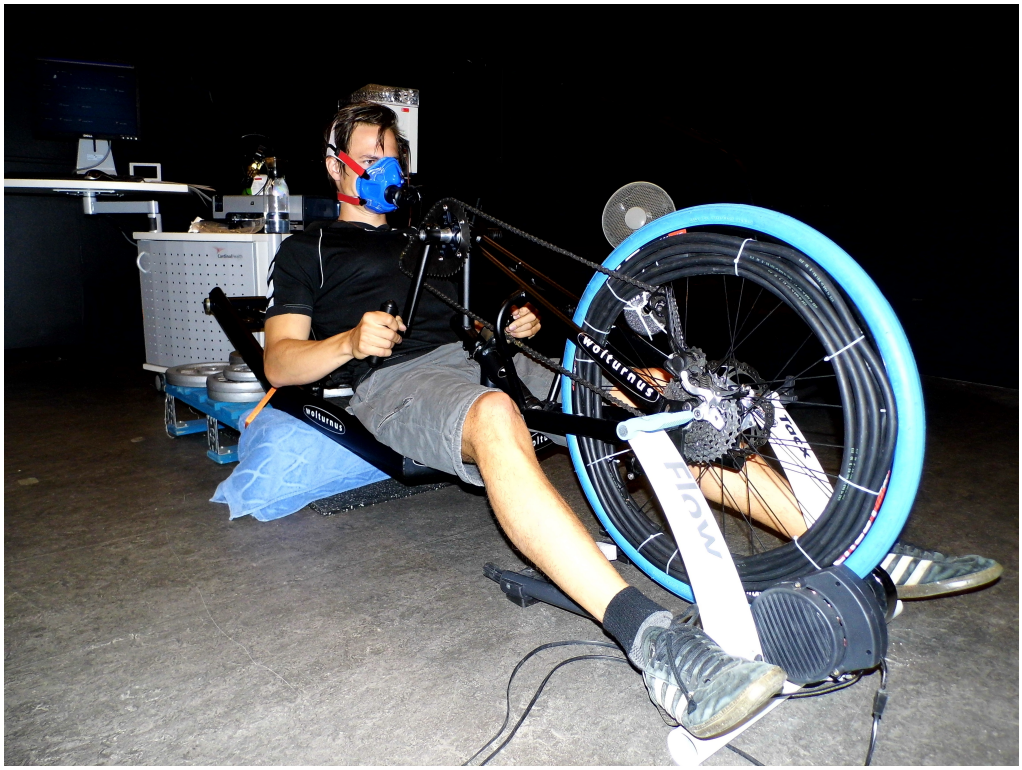

Figure 6.3: A view of the final laboratory setup when in use. The back wheels are replaced by a half euro pallet, weighted with 77 kg to stabilize the setup.

6.2 Data Processing: Experiment

Here is shown some more graphs and tables about the validation experiment.

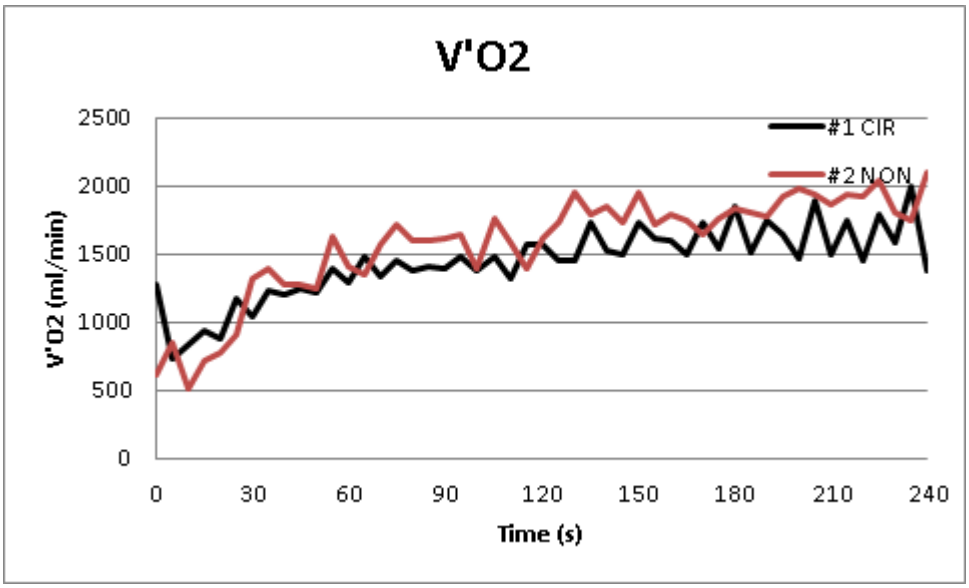

Figure 6.4: An example of the oxygen uptake for the two 4-min bouts. Statistics was only conducted on the last 60 s. Here, it is the data of subject G.

Subject	Mean O_2 CIR $(ml \cdot min^{-1})$	Mean O_2 NON $(ml \cdot min^{-1})$
A	1735	1901
B	1760	1767
C	1770	1916
D	1824	1930
E	1842	1908
F	1844	1820
G	1657	1895
H	1778	1978
I	1996	1946
J	1289	1384
Mean	1750	1844
SD	184	173

Table 6.2: Mean oxygen uptake for the 10 inexperienced subjects in the last 60 s of the 4-min bouts.

Subject	Mean speed CIR ($m \cdot s^{-1}$)	Mean speed NON ($m \cdot s^{-1}$)
A	5.65	5.65
B	5.63	5.47
C	5.74	5.64
D	5.58	5.59
E	5.49	5.49
F	4.82	4.71
G	5.73	5.70
H	5.60	5.59
I	5.65	5.61
J	4.56	4.58
Mean	5.44	5.4
SD	0.41	0.41

Table 6.3: Mean speed for the 10 inexperienced subjects in the last 90 s of the 4-min bouts.